

# Causal Discovery from Incomplete Data: A Deep Learning Approach

Yuhao Wang<sup>1</sup>, Vlado Menkovski<sup>1</sup>, Hao Wang<sup>2</sup>, Xin Du<sup>1</sup>, Mykola Pechenizkiy<sup>1</sup>

<sup>1</sup>Eindhoven University of Technology, <sup>2</sup>Massachusetts Institute of Technology  
{y.wang9, v.menkovski, x.du, m.pechenizkiy}@tue.nl, hoguewang@gmail.com

## Abstract

As systems are getting more autonomous with the development of artificial intelligence, it is important to discover the causal knowledge from observational sensory inputs. By encoding a series of cause-effect relations between events, causal networks can facilitate the prediction of effects from a given action and analyze their underlying data generation mechanism. However, missing data are ubiquitous in practical scenarios. Directly performing existing casual discovery algorithms on partially observed data may lead to the incorrect inference. To alleviate this issue, we proposed a deep learning framework, dubbed Imputed Causal Learning (ICL), to perform iterative missing data imputation and causal structure discovery. Through extensive simulations on both synthetic and real data, we show that ICL can outperform state-of-the-art methods under different missing data mechanisms.

## 1 Introduction

Analyzing causality is a fundamental problem to infer the causal mechanism from observed data. Usually causal relations among variables are described using a Directed Acyclic Graph (DAG), with the nodes representing variables and the edges indicating probabilistic relations among them. Learning such causal networks has proven useful in various applications, ranging from smart cities to health care. For example, knowledge of the causal structure is (1) helpful for analyzing relations among different business entities and supporting business decisions (Borboudakis and Tsamardinos 2016), (2) necessary in learning gene regulatory network and analyzing complex disease traits (Wang et al. 2017), (3) important for visualizing causal attentions of self-driving cars, where a highlighted region would causally influence the vehicular steering control (Lopez-Paz et al. 2017). In short, the discovered causal networks enable accurate decision making (Sulik, Newlands, and Long 2017), robust uncertainty inference (Nakamura, Loureiro, and Frery 2007), reliable fault diagnose (Cai, Huang, and Xie 2017), and efficient redundancy elimination (Xie and Chen 2017).

Previous works on causal discovery mainly focus on the complete-data setting. They either try to learn the Bayesian

network structure to estimate Markov properties or use the additive noise model for causal inference. However, causal discovery under the missing-data setting is still relatively under-explored (Gain and Shpitser 2018a). In practice, missing data is a common issue. The underlying missingness mechanisms can be categorized into three basic types: Missing At Random (MAR), Missing Completely At Random (MCAR), and Missing Not At Random (MNAR). For example, sensors on the road intersection can record the traffic density, and traffic related information will be transmitted to the Road Side Units (RSUs) for traffic management in real time. In MAR, missingness is caused by fully observed variables. For example, when the vehicle density is above a threshold, RSUs will get overloaded and fail to collect traffic data. Missing traffic data depends on the traffic density recorded by the traffic sensor. MCAR is a special case of MAR, the cause of missingness is purely random and does not depend on the variables of interest, such as the lost of traffic information happens by chance. In MNAR, missingness depends on either unobserved attributes or the missing attribute itself. For example, the missingness of RSUs depends on the traffic density detected by the sensor. Additionally, the sensor itself also introduces missing values.

Some of the previous approaches handling missing data by directly deleting data entries with missing values, resulting in a complete observation for the problem at hand (Carter 2006; Van den Broeck et al. 2015). This data processing way may be satisfactory with a small proportion of missing values (e.g., less than about 5% (Graham 2009)), but could result in a biased model in the presence of larger missing proportions. In theory, MCAR and MAR conditions ensure the recoverability of the underlying distributions from the measured value alone (Nakagawa 2015), and do not require the prior assumption of how data are missing. Therefore, a feasible solution can be first performing imputation to recover the missing entries, then followed by a causal discovery algorithm for knowledge representation from the recovered data (Strobl, Visweswaran, and Spirtes 2018). However, as will be discussed further, directly perform imputation could introduce incorrect causal relations.

In this paper, we focus on causal discovery from observational data (as opposed to intervention experiments). Note that estimating the causal graph as a DAG is an NP-complete problem (Chickering 1996), and the task becomes

even more challenging under the missing data condition. Causal discovery is an unsupervised learning problem and the goal is to discover the data generation process in the form of causal graphs. Inspired by (Yu et al. 2019) and motivated by the recent success of Generative Adversarial Networks (GAN) (Goodfellow et al. 2014) and Variational Autoencoder (VAE) (Diederik, Welling, and others 2014) in learning high-dimensional distributions, in this work, we use GAN and VAE to decompose this problem into two sub-problems, namely, iterative imputation with causal skeleton learning, and identify individual pairs of causal directions. In general, causal skeleton learning returns a reasonable network structure and offers a global view of how variables are dependent on each other, while causal direction identification provides a more accurate local view between the matched variable pairs. These complimentary local and global view helps approximate the data generating process among all observed variables.

Our contribution is three-fold:

- We propose a deep learning framework, called Imputed Causal Learning (ICL), for iterative missing data imputation and causal structure discovery, producing both imputed data and causal skeletons.
- We leverage the extra asymmetry cause-effect information within dependent pair sets in the causal skeleton  $\tilde{\mathcal{G}}$ . The causal directions in  $\tilde{\mathcal{G}}$  then being enumerated in a pair-wise way to uncover the underlying causal graph  $\mathcal{G}$ .
- Through extensive simulations on both synthetic and publicly-used real data, we show that under MCAR and MAR conditions, our proposed algorithm outperforms state-of-the-art baseline methods.

## 2 Related Work

**Causal Discovery from Complete Data** Methods for identifying causal relations from complete observation data usually fall into two categories: the first one exploits Markov properties of DAGs (Chickering 2002), and the second one tries to leverage asymmetries between variable pairs of the Functional Causal Model (FCM) (Shimizu et al. 2006; Mooij et al. 2016). For methods in the first category, they may not be able to orient the causal direction of  $X - Y$ , since  $X \rightarrow Y$  and  $Y \rightarrow X$  are Markov equivalent. However, the causal direction can be further identified using methods in the second category by leveraging the asymmetry between causes and effects. Methods in the first category typically include constraint-based approaches, score-based approaches, and hybrid approaches. They can discover the dependence relations and identify the Markov equivalence class. **Constraint-based approach** discovers conditional independence between variables of DAGs. Typical algorithms under this category include the PC algorithm, Fast Causal Inference (FCI) (Spirtes, Glymour, and Scheines 2000), and Really Fast Causal Inference (RFCI) (Colombo et al. 2011). Greedy Equivalence Search (GES) (Nandy et al. 2018) is a **Score-based approach**, it performs structure learning with a scoring criteria over the search space of the Markov Equivalence class. The recent breakthrough (Zheng et al. 2018) makes the score-based method amenable with

the existing black-box solvers. DAG-GNN (Yu et al. 2019) learns the DAG structure using a graph neural network. Besides, **hybrid approaches**, such as the the Adaptively Restricted Greedy Equivalence Search (ARGES) (Nandy et al. 2018), Causal Generative Neural Network (Goudet et al. 2018), which combine ideas of constraint and score-based approach. They restricts the score-based search space with the help of the conditional independence graph for either the computational efficiency or performance accuracy. Meanwhile, methods in the second category can be used to identify the causal directions, include linear non-Gaussian acyclic model (LiNGAM) (Shimizu et al. 2006), Addictive Noise Model (ANM) (Peters et al. 2014), Post-nonlinear model (PNL) (Zhang et al. 2016).

**Causal Discovery from Incomplete Data** Works related to causal discovery from incomplete data can be classified into two categories: one category attempts to discover causal structure using only available partial observations and the other aims at imputing all missing entries to recover the whole observation. Typical algorithms with partial observations perform (1) list-wise deletion on all entries (rows) with missing values before causal discovery (Gain and Shpitser 2018b). (2) Test-wise deletion effectively ignores only the variables containing missing values involved in the conditional independence (CI) test (Strobl, Visweswaran, and Spirtes 2018; Tu et al. 2019). These methods are suitable when the missingness mechanism can not be ignored and the underlying distribution is less likely to be recovered. Another category attempts to impute the missing values before performing causal discovery. Previous works use Expectation Maximization (EM) or Gibbs sampling to perform imputation. However, these approaches require prior knowledge of the underlying structure and are therefore not practical (Singh 1997). On the other hand, imputation strategies for handling missing data is also very important. Works related to this category include the Multivariate Imputation by Chained Equations (MICE) (White, Royston, and Wood 2011), MissForest (MF) (Stekhoven and Bühlmann 2011), and deep-learning-based approaches, such as using GAN for more powerful imputation (Li, Jiang, and Marlin 2019; Luo et al. 2018; Yoon, Jordon, and Schaar 2018). In this context, recovering the full distributions from missing data through imputation and performing causal discovery on the recovered data is the most straightforward solution (Adel and de Campos 2017).

## 3 Imputed Causal Learning

On a high level, our model first takes incomplete observational data  $\bar{X}$  as input and then simultaneously performs missing data imputation and structural learning to estimate both the causal skeleton (as an undirected graph) and the recovered data  $(\tilde{\mathcal{G}}, \hat{X})$  (Module A and B of Figure 1). After that, pair-wise causal direction identification is performed to orient the causal edges and uncover the final underlying causal graph  $\mathcal{G}$  (Module C of Figure 1). Figure 1 shows an overview of our framework. The following subsections explain these two steps in detail.

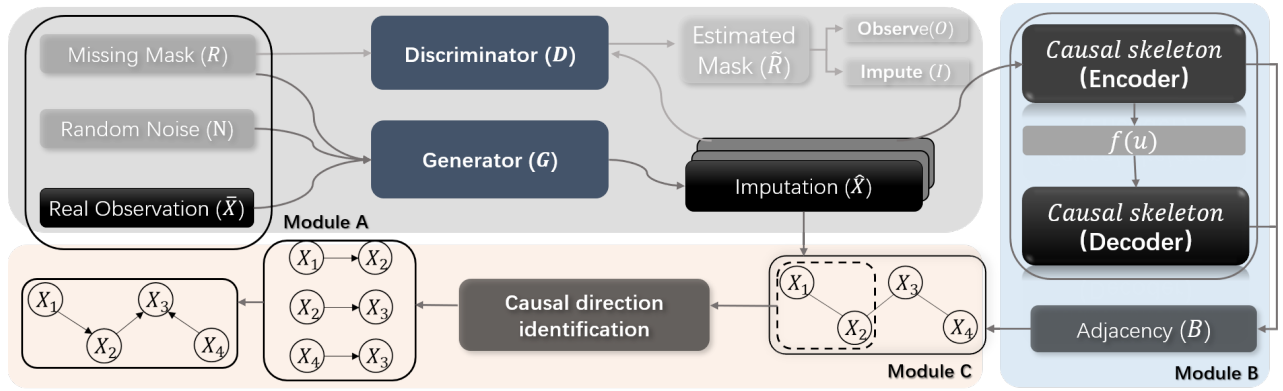


Figure 1: System architecture of our proposed ICL network, including three modules. We train Module A and B in an end-to-end manner for simultaneously imputation and causal skeleton learning, and the results is used as the input of Module C for causal direction identification.

**Notation and Preliminaries** A causal graph  $\mathcal{G} = (\mathcal{V}, \mathcal{E})$  consists of nodes  $\mathcal{V}$  and edges  $\mathcal{E}$ . We denote a random variable set  $X$  with  $X := (X_1, X_2, \dots, X_d)$ ,  $X \in \mathbb{R}^{n \times d}$  to represent  $n$  i.i.d. observations into an  $n \times d$  data matrix. Node set  $\mathcal{V}$  corresponds to  $d$  vertices, whereby each node  $i \in \mathcal{V}$  in  $\mathcal{G}$  represents a random variable  $X_i$  in a causal DAG. Within the edge set  $\mathcal{E}$ , an edge from two adjacent nodes  $X_i$  to  $X_j$  exists if and only if  $(i, j) \in \mathcal{E}$  and  $(j, i) \notin \mathcal{E}$ , leading to a cause-effect pair of  $X_i \rightarrow X_j$ . A causal skeleton can be represented as  $\bar{X}_i - X_j$ . Besides, linear causal relationship in a form of graph  $\mathcal{G}$  can be equivalently represented as a linear Structural Equation Model (SEM):

$$X_j = \sum_{K \in pa_j^{\mathcal{G}}} \beta_{ij} X_i + u_j \quad (j = 1, \dots, d). \quad (1)$$

And the relations between variables in rows are equivalent to  $X = B^T X + U$ .  $B \in \mathbb{R}^{d \times d}$  is a strictly upper triangular adjacency matrix with  $B_{i,i} = 0$  for all  $i$ , and  $B_{i,j} \neq 0$  represent an edge between  $X_i$  and  $X_j$  in  $\mathcal{G}$ .  $U$  is an  $n \times d$  noise matrix with noise vectors  $U := (u_1, u_2, \dots, u_d)$ . Furthermore, a generalized nonlinear SEM model can be formulated as  $X = B^T f(X) + U$  (Yu et al. 2019).  $B^T$  can be treated as an autoregression matrix of the DAG. The joint probability distribution  $P(X)$  is defined over the graphical model with a finite set of vertices  $\mathcal{V}$  on random variables  $X$ .

### 3.1 Causal Skeleton Discovery from Incomplete Data

**Problem Formulation and Method Overview** Under the missing data condition, we assume confounders (unobserved direct common cause of two variables) do not exist in the input data. This means that we can observe all variables but some samples may be missed. We define an incomplete version of  $X$  as  $\bar{X} := (\bar{X}_1, \bar{X}_2, \dots, \bar{X}_d)$ , where  $R = (R_1, R_2, \dots, R_d)$  in Equation (2) is the corresponding masks.  $R \in \{0, 1\}^d$  is a binary random variable and used to denote which entries in  $\bar{X}$  are missing. Specifically:

$$\bar{X}_i = \begin{cases} X_i, & \text{if } R_i = 1; \\ *, & \text{otherwise,} \end{cases} \quad (2)$$

where  $*$  means ‘missing’.

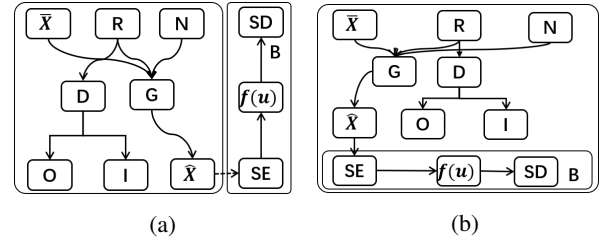


Figure 2: Incomplete data causal structure discovery (a) Imputation first, then structure discovery; (b) Simultaneous imputation and structure learning;

In this paper, causal skeleton discovery from incomplete data refers to the problem of inferring  $B$  from incomplete observations  $\bar{X}$ . We do this by iteratively imputing  $\bar{X}$  and updating  $B$ .

**Imputing  $\bar{X}$ :** Note that unlike previous causal discovery approaches dealing with missing data by either list-wise or test-wise deletion, we aim to generate full observations and yield an optimistic estimation from  $\bar{X}$  by imputation. Therefore, with  $\bar{X}$  only, we then need to first recover the underlying joint probability distribution  $P(X)$  from  $\bar{X}$ , and representing  $P(\bar{X})$  with a structured dependency among variables in  $\bar{X}$  with  $P(\bar{X}) = \prod_i P(\bar{X}_i | PA_i)$ , where  $PA_i$  denotes the set of parents of node  $i$ . We denote the recovered data by  $\hat{X} \in \mathbb{R}^{n \times d}$ , and then formulate our task as minimizing the distribution difference of  $P(X)$  and  $P(\bar{X})$  by imputing all missing values of  $\bar{X}$  into  $\hat{X}$ .

**Updating  $B$ :** In each iteration after imputing  $\bar{X}$ , we infer (and update) the autoregression parameter  $B$  with  $\hat{X} = B^T f(\hat{X}) + U$  by mapping samples from  $\hat{X}$  into a linear-separable hyperspace of  $f(\hat{X})$  with a neural network.

**Iterative Update:** The imputation (Module A of Figure 1) and learning of  $B$  (Module B of Figure 1) are performed jointly. This is important since the data imputation and learning of  $B$  can adjust and improve each other.

**Proposed Method** Built on GAN and VAE, we generalize the work on Bayesian structure learning from (Yu et al. 2019) and propose a deep learning algorithm to simultaneously perform missing data imputation and causal skele-

ton discovery. Our algorithm consists of four components: a generator ( $G$ ), a discriminator ( $D$ ), a structure encoder ( $SE$ ), and a structure decoder ( $SD$ ). Given incomplete observational data  $\bar{X}$ ,  $G$  and  $D$  learn to obtain the estimated complete data  $\hat{X}$ , based on which  $SE$  and  $SD$  will try to learn the causal structure  $B$ . These four components are trained jointly using backpropagation (BP).

Note that a naive approach would be to perform imputation first and then follow by causal discovery (Figure 2(a)). This is sub-optimal because the estimated causal discovery cannot improve the data imputation process in turn. Empirically we find that its performance is very similar to performing causal discovery after directly deleting all data entries with missing values, meaning that imputation does not introduce any additional value into the causal discovery process. We address this issue by alternating between imputation and causal discovery, which is made possible through the use of differentiable neural networks (Figure 2(b)). Such an iterative process can do better in terms of performing multiple imputation passes to take into account the variability while preserving the underlying statistical causal relationship between variables.

Concretely, in each iteration of our algorithm,  $G$  and  $D$  take the incomplete data as input and impute the missing values to form  $\hat{X}$ . The causal structure  $B$  is involved as parameters of both  $SE$  and  $SD$ . We encode  $\hat{X}$  into a latent code  $f(U)$  through  $SE$ , and decode  $f(U)$  into  $\tilde{X}$  with  $SD$ . The above procedure can be seen as two neural network modules, GAN and VAE, jointly learning together. The former recovers missing data while the later discovers the causal structure.

**Missing Data Imputation** Similar to (Luo et al. 2018; Yoon, Jordon, and Schaar 2018), we use  $G$  and  $D$  together to approach the underlying data distribution of  $P(X)$  for imputation. Since GAN can not take  $NaN$  values as the input, to initialize the imputation process, we use a  $d$ -dimensional noise variable  $N = (N_1, N_2, \dots, N_d)$  sampled from the standard normal distribution  $N \sim \mathcal{N}(\mathbf{0}, \mathbf{I})$ . And we replace the  $NaN$  entries in  $\bar{X}$  with  $\tilde{X} = R \odot \bar{X} + (1 - R) \odot N$ , where  $\odot$  represent element-wise multiplication.  $\tilde{X}$  will be served as the input of GAN to generate  $\hat{X}$ . With  $\hat{X}$  as the input of the structure learning neural network of  $SE$  and  $SD$  to discover the autoregression parameter  $B^T$  through each iteration (details of the structure learning method will we covered in the next subsection). Specifically, the generator is responsible for observing the real data and imputing missing components conditioned on what is actually observed according to  $P(\hat{X}|\bar{X})$ . The generator takes  $\bar{X}$ ,  $R$ , and  $N$  as input:

$$\hat{X} = G(R, \bar{X}, (1 - R) \odot N). \quad (3)$$

Therefore, the recovered data  $\hat{X}$  can be obtained by replacing data on missing entries in  $\bar{X}$  with the generated corresponding values from  $\hat{X}$  as

$$\hat{X} = R \odot \bar{X} + (1 - R) \odot \tilde{X}. \quad (4)$$

Besides, the discriminator  $D$  is introduced as an adversary training module accompanying the generator  $G$ . Due

to the incomplete observations, the initialized data  $\bar{X}$  inherently contains both real and fake values, which makes  $D$  from standard GAN not feasible for our task. In this context, instead of counting real/fake from  $\bar{X}$ , the mapping of  $D(\cdot)$  attempts to determine whether the components are actually observed or not. Specifically, we set  $\hat{X}$  as the input to  $D$ , while  $G$  is trying to fool  $D$  in an adversarial way. In summary,  $G$  and  $D$  together learn a desired joint distribution of  $P(\hat{X})$  and then perform imputation given  $\bar{X}$ . Note that the difference between ICL and previous GAN-based imputation methods is that our imputation is also related to the recovered causal skeleton.

**Causal Skeleton Learning** Then we perform structure discovery to find the underlying causal mechanism from the variable set  $\mathcal{V}$  in  $\hat{X}$ . Using the structure discovery method in (Yu et al. 2019), with the scoring function  $\mathcal{S}_{\mathcal{D}}$ , this concatenate task then turns into a continuous optimization problem of finding a  $\tilde{\mathcal{G}}$  that satisfies:

$$\begin{aligned} \tilde{\mathcal{G}} &= g(\argmin_{\mathcal{G} \in \mathbb{R}^{d \times d}} \mathcal{S}_{\mathcal{D}}(\mathcal{G})), \\ \text{s.t. } h(\mathcal{G}) &= \text{tr}[(I + \alpha B \circ B)^d] - d = 0, \end{aligned} \quad (5)$$

where  $g(\cdot)$  is a function to remove directions in  $\mathcal{G}$ , leading to predicted causal skeleton  $\tilde{\mathcal{G}}$ . The adjacency matrix space  $\mathbb{R}^{d \times d}$  represents the set of all DAGs.  $h : \mathbb{R}^{d \times d} \rightarrow \mathbb{R}$  is the smooth function over real matrices, and  $h(\mathcal{G}) = 0$  ensures that  $\mathcal{G}$  is acyclic.  $\alpha$  is a hyperparameter. Following (Yu et al. 2019),  $SE$  takes  $\hat{X}$  as the input of a multilayer perceptron (MLP). The output, denoted as  $MLP(\hat{X}, \mathbf{W}_1)$ , is then multiplied by  $(I - B^T)$  and transformed into  $f(U)$  in Equation (6), where  $U$  is the noise vector mentioned at the start of Section 3. The decoder  $SD$  in Equation (7) performs an inverse operation  $(I - B^T)^{-1}$  on the encoded  $f(U)$  to recover  $\tilde{X}$ , where  $B$  is a parameter of  $SE$  and  $SD$  to incorporate the causal structure during the learning process.  $I$  denotes the identity matrix.  $\mathbf{W}_1$  and  $\mathbf{W}_2$  are parameters in corresponding layers.

$$f(U) = (I - B^T)MLP(\hat{X}, \mathbf{W}_1); \quad (6)$$

$$\tilde{X} = MLP((I - B^T)^{-1}(f(U), \mathbf{W}_2)), \quad (7)$$

The parameter  $B$  plays an important role during the learning phase,  $B_{i,j} \neq 0$  stands for the dependence relationship between  $X_i$  and  $X_j$  in  $\tilde{\mathcal{G}}$ .

By extracting  $B^T$  from the learning process described in Equations (6) and (7), we can have the knowledge of the marginal or conditional distribution of a random variable in  $\mathcal{V}$ . This is also how we discover a causal skeleton from  $\hat{X}$ .

**Joint Training** The overall procedure can be seen as simultaneously recovering all missing entries in  $\bar{X}$  by  $G$  and  $D$ , and optimizing the structure learning performance of  $P(\tilde{\mathcal{G}}|\hat{X}, R)$  by  $SE$  and  $SD$ .

The loss function is formed into two parts as the imputation loss and structure learning loss. Since the missing values in real-scene are not known, it would not make sense to use their reconstruction error as a stopping criterion in the imputation loss part. The training objective can be formulated as a

*minimax* problem of  $\min_G \max_D L_i(D, G)$  while measuring the degree of imputation fitness, as it is usually done when using the standard GANs. In our work, we optimize the data generation performance of a GAN with the loss function as follows

$$L_i(D, G) = \mathbb{E}_{\tilde{X}, R, N} [R^T \log D(G(R, \tilde{X}, (1-R) \odot N)) + (1-R^T) \log(1 - D(G(R, \tilde{X}, (1-R) \odot N)))] \quad (8)$$

The generator  $G$  generates samples conditioned on the partial observation of  $\tilde{X}$ , the missingness indicator  $R$ , and the noise  $N$ . We train  $G$  to generate  $\hat{X}$  and minimize the prediction probability of  $R$ , while we train  $D$  to maximize the prediction accuracy of  $R$ . Then we follow the evidence lower bound (ELBO) from (Yu et al. 2019), given below, for causal skeleton learning.

$$L_e = -\mathbb{E}_{q(U|\hat{X})} [\log p(\hat{X}|U)] + D_{KL}(q(U|\hat{X})||p(U))$$

We denote  $\Phi$  and  $\Theta$  as parameter sets in GANs and VAEs separately. The overall learning problem can be formed as:

$$\begin{aligned} \min_{\Phi} f(\Phi) &= L_i(G, D); \\ \min_{B, \Theta} f(B, \Theta) &= -L_e, \text{ s.t. } h(B) = 0. \end{aligned} \quad (9)$$

The stopping criteria is either the error is sufficiently small or the number of iterations is large enough. With the best fitting  $B$  in Equation (9), the causal skeleton  $\tilde{\mathcal{G}}$  is generated by keeping edges in  $\mathcal{E}$  but remove their directions. The pseudo code is summarized in Algorithm 1.

---

#### Algorithm 1: Causal Skeleton Discovery

---

**Initialize** :  $R \in \{0, 1\}^{n \times d}$ ,  $\tilde{X} \in \mathbb{R}^{n \times d}$ ,  $\tilde{\mathcal{G}} \in \mathbb{R}^{d \times d}$ ,  
 $N = P_n \sim \mathcal{N}(\mu, \sigma^2)$ , minibatch  $J$ .  
**Input** : Observational incomplete data  $\tilde{X}$ .  
**Output** : Causal skeleton and imputed data  $(\tilde{\mathcal{G}}, \hat{X})$ .  
**while** Loss has not converged **do**  
  **for**  $j = 1 : J$  **do**  
    **Step 1: Missing data imputation:**  
    Missing entries:  $\tilde{X} = G(R, \tilde{X}, (1-R) \odot N)$ .  
    Imputation:  $\hat{X} = R \odot \tilde{X} + (1-R) \odot \tilde{X}$ .  
    **Step 2: Structure discovery:**  
    SE:  $f(U) = (I - B^T)MLP(\hat{X}, \mathbf{W})$ .  
    SD:  $\tilde{X} = MLP((I - B^T)^{-1}(f(U), \mathbf{W}))$ .  
    **Step 3: Extract  $\mathcal{G}$  from  $B$ :**  
    Let  $\tilde{\mathcal{G}} = (\mathcal{V}, \mathcal{E})$  with  $\mathcal{E} = \{(i, j) : B_{i,j} \neq 0\}$ .  
    **Step 4: Update parameters  $\Phi$  of  $G$  and  $D$  in GAN**  
    using SGD according to Equation (8).  
    **Step 5: Update parameters  $\Theta$  of SE and SD in VAE**  
    and  $B$  using SGD according to Equation (9).  
  **end**  
**end**

---

### 3.2 Causal Direction Identification

The above procedure can identify the conditional probability, but may not truly represent the underlying causal mechanism. For example, given two variables  $X_i$  and

$X_j$ , their joint distribution  $P(X_i, X_j)$  can be decomposed equally as either  $P(X_j|X_i)P(X_i)$  ( $X_i \rightarrow X_j$ ) or  $P(X_i|X_j)P(X_j)$  ( $X_j \rightarrow X_i$ ). These two decompositions relate to different causal mechanisms. With the additive noise model (Mooij et al. 2016)  $\hat{X}_j = f(\hat{X}_i) + U$ ,  $U \perp\!\!\!\perp \hat{X}_i$ , however, we can represent asymmetries between  $X_i \rightarrow X_j$  and  $X_j \rightarrow X_i$ , leading to a unique causal direction from purely observational data. In detail, let the joint distribution of  $P(\hat{X}_i, \hat{X}_j)$  with ground truth be  $\{(\hat{X}_i \rightarrow \hat{X}_j), (i, j) \in d\}$ . Then the effect of  $X_j$  conditioned on the cause  $X_i$  can be represented by:

$$\begin{aligned} P(\hat{X}_j = x_j^m | \hat{X}_i = x_i^m) &= \frac{P(\hat{X}_j = x_j^m, \hat{X}_i = x_i^m)}{P(X_i = x_i^m)} \\ &\stackrel{x_i \perp\!\!\!\perp U}{x_j \not\perp\!\!\!\perp U} \frac{P(U = x_j^m - f(x_i^m))P(X_i = x_i^m)}{\mathbb{P}(X_i = x_i^m)} \\ &= P(U = x_j^m - f(x_i^m)) \\ &= P(U = \epsilon), (X_i \rightarrow X_j, (i, j) \in d, m \in n), \end{aligned} \quad (10)$$

where the second equality assumes  $X_j \not\perp\!\!\!\perp N$  and  $X_i \perp\!\!\!\perp N$ . Note that due to the asymmetry, Equation (10) does not hold in the reverse direction  $X_j \rightarrow X_i$ . This property makes it possible to determine the causal direction from observational data under proper conditions.

Therefore, given  $(\tilde{\mathcal{G}}, \hat{X})$  from the above section, our goal is to utilize such pair-wise asymmetry and orient the edges of  $\tilde{\mathcal{G}}$ , consequently uncovering the final causal DAG  $\mathcal{G}$ . This can be achieved by calculating the maximum evidences of the marginal log-likelihood over two models  $M(X_i, X_j)$  and  $M(X_j, X_i)$ . The model that shows the larger evidence is selected. In this work, we use the Cascade Additive Noise Model (CANM) proposed by (Cai et al. 2019). Specifically, to enumerate causal direction from variables pairs in  $\tilde{\mathcal{G}}$ , we use variable pairs  $\hat{X}(x_i^m, x_j^m)$  from  $\hat{X}$  as input, then the log-marginal likelihood on variable  $X_i$  and  $X_j$  is computed with:

$$\begin{aligned} \log p_{\theta}(X_i, X_j) &= \log \prod_{m=1}^n \int p_{\theta}(\hat{x}_i^m, \hat{x}_j^m, z) dz \\ &:= \sum_{m=1}^n \mathcal{L}(\theta, \phi; \hat{x}_i^m, \hat{x}_j^m) + KL(q_{\phi}(z|\hat{x}_i^m, \hat{x}_j^m) \parallel p_{\theta}(z|\hat{x}_i^m, \hat{x}_j^m)) \\ &\geq \sum_{m=1}^n \mathcal{L}(\theta, \phi; \hat{x}_i^m, \hat{x}_j^m). \end{aligned}$$

$\theta$  and  $\phi$  are the parameters of the CANM model, which encode  $\hat{x}_i^m$  and  $\hat{x}_j^m$  into a latent code  $z$ . The evidence score  $S_{x_i \rightarrow x_j}$  of the log marginal likelihood with  $\sum_{m=1}^n \mathcal{L}(\theta, \phi; \hat{x}_i^m, \hat{x}_j^m)$  can be calculated in the following way in both directions.

$$\sum_{m=1}^n E_{z \sim q_{\phi}(z|x_i, x_j)} [-\log q_{\phi}(z|x_i, x_j) + \log p_{\theta}(x_i, x_j, z)].$$

And the causal direction can be identified by:

$$\text{dir} := \begin{cases} \hat{X}_i \rightarrow \hat{X}_j, & \text{if } \hat{S}_{x_i \rightarrow x_j} > \hat{S}_{x_j \rightarrow x_i} \\ \hat{X}_j \rightarrow \hat{X}_i, & \text{if } \hat{S}_{x_i \rightarrow x_j} < \hat{S}_{x_j \rightarrow x_i} \\ \text{Not determined.} & \text{others} \end{cases} \quad (11)$$

Given the bivariate identifiable condition in Equation (10), causal discovery from more than two variables can be achieved if each of the causal pairs follows the ANM class (Peters et al. 2011). To uncover the underlying causal graph  $\mathcal{G}$ , we then independently orient each pair-wise edge using the bivariate identification method in Equation (11). Besides, note that a combination of causal structure learning and bi-variate direction identification requires a final verification to ensure that the DAG is acyclic. In the final stage, by checking if cycles  $\mathcal{G}_C$  in  $\mathcal{G}$  exist, we enumerate the related edges with the calculated score  $(\mathcal{E}_{ij}, S_{x_i, x_j})$ , then simply remove the edge which holds the lowest score. We will consider more sophisticated algorithms in future work.

## 4 Experiment Results

In this section, we will demonstrate how ICL performs on two synthetic datasets and one real-world dataset compared to state-of-the-art baselines.

### 4.1 Baseline Algorithms

Algorithms for data imputation include list-wise deletion (LD), multivariate imputation by chained equations (MICE) (White, Royston, and Wood 2011), MissForest (MF) (Stekhoven and Bühlmann 2011), and GAN from as shown in Figure 2(a). Algorithms for the causal structure discovery include **constraint-based approaches** such as PC (Spirtes, Glymour, and Scheines 2000), linear non-Gaussian acyclic model (LiNGAM) (Shimizu et al. 2006), really fast causal inference (RFCI) (Colombo et al. 2011), **score-based approaches** such as greedy equivalence search (GES) (Chickering 2002), **hybrid approaches** such as max-min parents-children-addictive noise model (MMPC-ANM) (Cai et al. 2018), and a deep-learning approach based on DAG-GNN (Yu et al. 2019). For DAG-GNN we consider two variants: GAN-DAG first performs imputation first and then use the imputation results for structure discovery; LD-DAG first delete all entries with missing values and then perform causal discovery. Each baseline consists of one data imputation algorithm and one causal discovery algorithm. Therefore we have the following combinations: LD-PC, LD-LiNGAM, LD-RFCI, LD-MMPC, LD-GES; MF-PC, MF-LiNGAM, MF-RFCI, MF-MMPC, MF-GES; MC-PC, MC-LiNGAM, MC-RFCI, MC-MMPC, MC-GES; GAN-PC, GAN-LiNGAM, GAN-RFCI, GAN-MMPC, GAN-GES. All the baseline algorithms above are implemented using R-packages such as **bnlearn** (Scutari 2009), **CompareCausalNetworks** (Heinze-Deml and Meinshausen 2017), **pcalg** (Kalisch et al. 2012), and **SELF** (Cai et al. 2018). We use **rrpy2** (Gautier 2012) to make the above R-packages accessible from Python and ensure that all algorithms can be compared in the same environment. Following (Tu et al. 2019; Strobl, Visweswaran, and Spirtes 2018), we use Structural Hamming Distance (SHD) as the evaluation metric.

### 4.2 Quantitative Results

In this subsection, we first provide on synthetic and real-world datasets in terms of both the causal graphs and the missing mechanisms. We then compare ICL with the baselines above on these datasets.

**Synthetic Data Generation** The synthetic ground truth graph  $\mathcal{G}$  with  $d$  nodes is generated randomly using the Erdős Rényi (ER) model with an expected neighbor size  $s = 2$ . The edge weights of  $\mathcal{G}$  are uniformly drawn from  $B \sim U(-2, -0.5] \cup U[0.5, 2)$  to ensure that they are non-zero. Once  $\mathcal{G}$  is generated, the observational i.i.d. data  $\bar{X} \in \mathbb{R}^{n \times d}$  is generated with a sample size  $n = \{500, 1000\}$  and a variable size  $d \in \{30, 50\}$ . For linear cases, the i.i.d. data is generated by sampling the model  $X = B^T X + N$ , where  $B$  is a strictly upper triangular matrix; similarly for nonlinear cases, the sampled model is described by  $X = f(B^T X) + N$ . Here the noise  $N$  follows either the Exponential or the Gumbel distribution. In our work, two different mechanisms are considered in nonlinear cases:

- 1 :  $x = 2\sin(B^T(x + 0.5 \cdot 1)) + B^T(x + 0.5 \cdot 1) + u$ ,
- 2 :  $x = \sqrt{x(B^T(x^2 + 0.5 \cdot 1))} + u$ .

In order to achieve a more general comparison in our experiments, the missing data proportions over all the synthetic data are set to be 10%, 30%, and 50%.

**Missingness Mechanisms** In this paper we generate synthetic incomplete data using one of the two missingness mechanisms, namely MCAR and MAR, leaving MNAR as future work. For MCAR, the missingness mask  $R \in \mathbb{R}^{n \times d}$  is formed by selecting the missing entries from the observational data corresponding to  $t_i < \tau$  ( $t_i \in T$ ) with the same probability. Here  $T \in \mathbb{R}^{n \times d}$  is a uniformly distributed random matrix which has the same dimensions as the observational data matrix. A threshold  $\tau$  is used as the missingness selection criterion. For MAR, the missingness mask  $R \in \mathbb{R}^{n \times d}$  is generated based on both the randomly generated graph  $\mathcal{G}$  (more details later) and  $T$ . Specifically, we first randomly sample parent-child pairs, denoted as  $S_p = \{(i, j)\}$ , from  $\mathcal{G}$ .  $R_{kj}$  is then set to 0 if there exists an  $i$  such that  $(i, j) \in S_p$  and  $T_{ki} < \tau$ . This is to simulate the setting where the missingness of the child node is determined by the (randomly generated) values of its parent nodes.

**Quantitative Experiment Results** Table 1 reports SHD of our proposed ICL and other baselines. The results are averaged over twenty random repetitions, with the missing proportion  $m \in \{10\%, 30\%, 50\%\}$  and under both MCAR and MAR conditions. We cover two nonlinear mechanisms as mentioned above. In our experiments, the linear results are consistent with the nonlinear results, and are not included due to space constraints. As shown in Table 1, ICL shows superior performance compared with all other baselines. 'Ideal SHD' refers to ICL's performance using *complete* data (no missing values). Recall that GAN-DAG performs data imputation first and then follow by data causal discovery without the iterative process. As shown in Table 1, GAN-DAG's performance is worse than ICL since its causal module cannot improve the data imputation process in turn. Interestingly, comparing LD-DAG and ICL, we can see that ignoring entries with missing values may have a negative effect on the performance of causal discovery. Furthermore, GES-based algorithms achieve the worst performance even with only 10% missing values. We can also see that MMPC-based

Table 1: Performance comparison (mean and standard deviation) using Structural Hamming Distance, lower is better.

		30 Var MCAR (Nonlinear 1) (Ideal SHD=7)			50 Var MAR (Nonlinear 2) (Ideal SHD=17)		
		10%	30%	50%	10%	30%	50%
GES	LD-GES	106.0 $\pm$ 14.3	109.1 $\pm$ 16.9	145.4 $\pm$ 13.4	227.2 $\pm$ 22.5	224.1 $\pm$ 28.6	225.6 $\pm$ 28.4
	GAN-GES	107.8 $\pm$ 12.2	106.9 $\pm$ 14.8	133.1 $\pm$ 15.9	228.5 $\pm$ 21.3	224.2 $\pm$ 25.6	225.6 $\pm$ 27.8
	MF-GES	109.3 $\pm$ 13.8	108.1 $\pm$ 14.8	136.9 $\pm$ 16.1	230.6 $\pm$ 21.6	224.1 $\pm$ 28.5	223.9 $\pm$ 26.9
	MC-GES	109.3 $\pm$ 13.8	109.1 $\pm$ 15.2	132.3 $\pm$ 16.2	230.6 $\pm$ 21.6	225.4 $\pm$ 28.0	225.4 $\pm$ 27.2
RFCI	LD-RFCI	22.2 $\pm$ 5.2	26.4 $\pm$ 8.3	43.3 $\pm$ 7.4	44.1 $\pm$ 8.3	49.7 $\pm$ 8.8	68.2 $\pm$ 10.1
	GAN-RFCI	38.6 $\pm$ 5.1	39.9 $\pm$ 8.3	42.0 $\pm$ 7.3	52.3 $\pm$ 8.3	66.6 $\pm$ 8.7	69.2 $\pm$ 10.1
	MF-RFCI	38.9 $\pm$ 5.0	39.9 $\pm$ 8.3	44.6 $\pm$ 7.0	51.0 $\pm$ 8.4	66.7 $\pm$ 8.8	68.8 $\pm$ 9.7
	MC-RFCI	38.8 $\pm$ 4.8	39.8 $\pm$ 8.3	42.7 $\pm$ 7.1	51.7 $\pm$ 8.2	66.5 $\pm$ 9.1	69.0 $\pm$ 10.1
LiNGAM	LD-LiNGAM	22.0 $\pm$ 8.4	25.3 $\pm$ 10.3	32.6 $\pm$ 10.4	41.3 $\pm$ 15.2	50.4 $\pm$ 17.6	53.9 $\pm$ 7.1
	GAN-LiNGAM	20.9 $\pm$ 8.4	23.1 $\pm$ 10.3	37.0 $\pm$ 10.4	43.0 $\pm$ 15.2	53.2 $\pm$ 17.6	47.6 $\pm$ 7.1
	MF-LiNGAM	23.1 $\pm$ 7.8	23.5 $\pm$ 8.3	37.6 $\pm$ 11.2	52.0 $\pm$ 16.9	48.2 $\pm$ 18.1	52.4 $\pm$ 13.6
	MC-LiNGAM	21.5 $\pm$ 8.9	29.1 $\pm$ 12.3	37.3 $\pm$ 12.0	43.6 $\pm$ 13.1	51.9 $\pm$ 14.0	52.6 $\pm$ 11.2
PC	LD-PC	26.2 $\pm$ 6.2	27.9 $\pm$ 7.6	35.0 $\pm$ 6.4	36.0 $\pm$ 7.7	38.5 $\pm$ 10.4	45.2 $\pm$ 8.1
	GAN-PC	26.0 $\pm$ 6.2	26.1 $\pm$ 7.6	32.3 $\pm$ 6.4	34.2 $\pm$ 7.7	38.6 $\pm$ 10.4	41.6 $\pm$ 7.4
	MF-PC	26.4 $\pm$ 5.8	26.2 $\pm$ 7.9	33.3 $\pm$ 6.8	35.0 $\pm$ 8.0	35.3 $\pm$ 10.1	41.9 $\pm$ 7.0
	MC-PC	27.9 $\pm$ 5.9	26.8 $\pm$ 8.2	33.3 $\pm$ 7.2	34.7 $\pm$ 8.0	37.8 $\pm$ 10.9	42.2 $\pm$ 7.5
MMPC	LD-MMPC	22.6 $\pm$ 7.3	23.2 $\pm$ 7.5	30.7 $\pm$ 9.7	45.2 $\pm$ 11.4	44.5 $\pm$ 11.1	44.0 $\pm$ 7.0
	GAN-MMPC	22.0 $\pm$ 7.5	23.8 $\pm$ 7.2	27.0 $\pm$ 9.9	46.0 $\pm$ 11.1	48.5 $\pm$ 10.5	44.5 $\pm$ 6.5
	MF-MMPC	22.8 $\pm$ 7.3	25.0 $\pm$ 7.2	29.1 $\pm$ 9.6	46.3 $\pm$ 11.2	48.7 $\pm$ 11.2	44.5 $\pm$ 6.9
	MC-MMPC	22.4 $\pm$ 7.3	25.8 $\pm$ 7.2	29.4 $\pm$ 9.5	46.3 $\pm$ 11.1	48.6 $\pm$ 11.2	44.4 $\pm$ 7.1
DAG	LD-DAG	12.2 $\pm$ 6.2	13.6 $\pm$ 9.2	20.0 $\pm$ 10.4	30.2 $\pm$ 5.9	32.5 $\pm$ 4.5	37.9 $\pm$ 7.1
	GAN-DAG	11.0 $\pm$ 7.7	10.3 $\pm$ 6.8	14.4 $\pm$ 8.7	23.4 $\pm$ 5.5	27.7 $\pm$ 3.9	30.5 $\pm$ 4.2
	ICL (Ours)	<b>9.8 <math>\pm</math> 3.9</b>	<b>7.4 <math>\pm</math> 3.8</b>	<b>8.4 <math>\pm</math> 4.9</b>	<b>19.0 <math>\pm</math> 4.2</b>	<b>25.5 <math>\pm</math> 3.8</b>	<b>27.3 <math>\pm</math> 5.5</b>

algorithms are suitable for nonlinear data, while LiNGAM-based algorithms are suitable for linear data. As expected, directly removing the missing entries leads to worse performance, since it not only reduces the sample size (and consequently throwing away useful information in the observational data), but also introduced a form of selection bias, leading to incorrect causal discovery (Gain and Shpitser 2018b). Furthermore, it is also worth mentioning that by performing missing data imputation and causal discovery separately (like GAN-DAG), the results could be even worse than deletion-based methods. As we discussed, imputation could be helpful for recovering the joint distribution of  $P(X)$ , but sub-optimal when we want to perform a further step of the distribution decomposition to discover the underlying causal graph. In contrast, our ICL model does not have the issues above and can therefore achieve better performance.

**Case Study on AutoMPG** As a case study we also show ICL’s results on a real-world dataset, AutoMPG (Lichman and others 2013), which is a city-cycle fuel consumption dataset with 398 instances. We discard the attributes of the car-name and the origin, and use the left 7 attributes: miles per gallon consumption (MPG), the release date of vehicles (AGE), vehicle weight (WEI), engine displacement (DIS), cylinder number (CYL), horsepower (HP), and vehicle’s acceleration capability (ACC). We simulate 10% missing data under MAR and compare the performance of ICL and GAN-DAG (best baseline). Their learned causal networks are shown in Figure 3, where the SHD for ICL and GAN-DAG is 9 and 11, respectively.

## 5 Conclusion

In this work, we addressed the problem of incomplete data causal discovery, and we proposed a deep learning model of

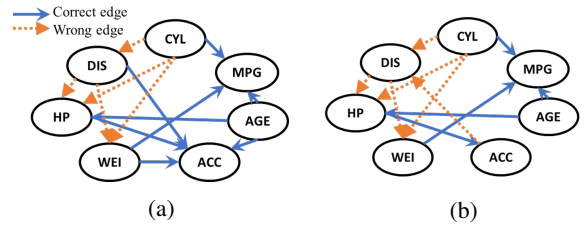


Figure 3: AutoMPG results. (a) Our ICL algorithm (SHD=9). (b) GAN-DAG (SHD=11).

ICL to handle this issue. Specifically, our ICL model contains a global view of iterative missing data imputation and causal skeleton discovery, and a local view of enumerating causal directions to uncover the underlying causal  $\mathcal{G}$ . In the end, we evaluated the effectiveness of our method on both synthetic and real data. As future work, we will generalize our method under more complex conditions such as the existence of confounders.

## References

- [Adel and de Campos 2017] Adel, T., and de Campos, C. P. 2017. Learning bayesian networks with incomplete data by augmentation. In *Thirty-First AAAI Conference on Artificial Intelligence*.
- [Borboudakis and Tsamardinos 2016] Borboudakis, G., and Tsamardinos, I. 2016. Towards robust and versatile causal discovery for business applications. *Proceedings of the 22nd ACM SIGKDD International Conference on Knowledge Discovery and Data Mining* 1435–14443.
- [Cai et al. 2018] Cai, R.; Qiao, J.; Zhang, Z.; and Hao, Z. 2018. Self: Structural equational likelihood framework for causal discovery. In *Thirty-Second AAAI Conference on Artificial Intelligence*.
- [Cai et al. 2019] Cai, R.; Qiao, J.; Zhang, K.; Zhang, Z.; and



- Hao, Z. 2019. Causal discovery with cascade nonlinear additive noise model. In *Proceedings of the Twenty-Eighth International Joint Conference on Artificial Intelligence, IJCAI-19*, 1609–1615. International Joint Conferences on Artificial Intelligence Organization.
- [Cai, Huang, and Xie 2017] Cai, B.; Huang, L.; and Xie, M. 2017. Bayesian networks in fault diagnosis. *IEEE Transactions on Industrial Informatics* 13(5):2227–2240.
- [Carter 2006] Carter, R. L. 2006. Solutions for missing data in structural equation modeling. In *Research & Practice in Assessment*, volume 1, 4–7. ERIC.
- [Chickering 1996] Chickering, D. M. 1996. Learning bayesian networks is np-complete. In *Learning from data*. Springer. 121–130.
- [Chickering 2002] Chickering, D. M. 2002. Optimal structure identification with greedy search. *Journal of machine learning research* 3(Nov):507–554.
- [Colombo et al. 2011] Colombo, D.; Maathuis, M. H.; Kalisch, M.; and Richardson, T. S. 2011. Learning high-dimensional dags with latent and selection variables. In *Proceedings of the Twenty-Seventh Conference on Uncertainty in Artificial Intelligence*, 850–850. AUAI Press.
- [Diederik, Welling, and others 2014] Diederik, P. K.; Welling, M.; et al. 2014. Auto-encoding variational bayes. In *Proceedings of the International Conference on Learning Representations (ICLR)*.
- [Gain and Shpitser 2018a] Gain, A., and Shpitser, I. 2018a. Structure Learning Under Missing Data. In Kratochvíl, V., and Studený, M., eds., *Proceedings of the Ninth International Conference on Probabilistic Graphical Models*, volume 72 of *Proceedings of Machine Learning Research*, 121–132. Prague, Czech Republic: PMLR.
- [Gain and Shpitser 2018b] Gain, A., and Shpitser, I. 2018b. Structure learning under missing data. In Kratochvíl, V., and Studený, M., eds., *Proceedings of the Ninth International Conference on Probabilistic Graphical Models*, volume 72 of *Proceedings of Machine Learning Research*, 121–132. Prague, Czech Republic: PMLR.
- [Gautier 2012] Gautier, L. 2012. rpy2: A simple and efficient access to r from python, 2012. URL <http://rpy.sourceforge.net/rpy2.html>.
- [Goodfellow et al. 2014] Goodfellow, I.; Pouget-Abadie, J.; Mirza, M.; Xu, B.; Warde-Farley, D.; Ozair, S.; Courville, A.; and Bengio, Y. 2014. Generative adversarial nets. In *Advances in neural information processing systems*, 2672–2680.
- [Goudet et al. 2018] Goudet, O.; Kalainathan, D.; Caillou, P.; Guyon, I.; Lopez-Paz, D.; and Sebag, M. 2018. Learning functional causal models with generative neural networks. In *Explainable and Interpretable Models in Computer Vision and Machine Learning*. Springer. 39–80.
- [Graham 2009] Graham, J. W. 2009. Missing data analysis: Making it work in the real world. *Annual review of psychology* 60:549–576.
- [Heinze-Deml and Meinshausen 2017] Heinze-Deml, C., and Meinshausen, N. 2017. Comparecausalnetworks: interface to diverse estimation methods of causal networks. *R package*.
- [Kalisch et al. 2012] Kalisch, M.; Mächler, M.; Colombo, D.; Maathuis, M. H.; Bühlmann, P.; et al. 2012. Causal inference using graphical models with the r package pcalg. *Journal of Statistical Software* 47(11):1–26.
- [Li, Jiang, and Marlin 2019] Li, S. C.-X.; Jiang, B.; and Marlin, B. 2019. Learning from incomplete data with generative adversarial networks. In *International Conference on Learning Representations*.
- [Lichman and others 2013] Lichman, M., et al. 2013. Uci machine learning repository.
- [Lopez-Paz et al. 2017] Lopez-Paz, D.; Nishihara, R.; Chintala, S.; Scholkopf, B.; and Bottou, L. 2017. Discovering causal signals in images. In *Proceedings of the IEEE Conference on Computer Vision and Pattern Recognition*, 6979–6987.
- [Luo et al. 2018] Luo, Y.; Cai, X.; Zhang, Y.; Xu, J.; et al. 2018. Multivariate time series imputation with generative adversarial networks. In *Advances in Neural Information Processing Systems*, 1596–1607.
- [Mooij et al. 2016] Mooij, J. M.; Peters, J.; Janzing, D.; Zscheischler, J.; and Schölkopf, B. 2016. Distinguishing cause from effect using observational data: methods and benchmarks. *The Journal of Machine Learning Research* 17(1):1103–1204.
- [Nakagawa 2015] Nakagawa, S. 2015. Missing data: mechanisms, methods and messages. *Ecological statistics: Contemporary theory and application* 81–105.
- [Nakamura, Loureiro, and Frery 2007] Nakamura, E. F.; Loureiro, A. A.; and Frery, A. C. 2007. Information fusion for wireless sensor networks: Methods, models, and classifications. *ACM Computing Surveys (CSUR)* 39(3):9.
- [Nandy et al. 2018] Nandy, P.; Hauser, A.; Maathuis, M. H.; et al. 2018. High-dimensional consistency in score-based and hybrid structure learning. *The Annals of Statistics* 46(6A):3151–3183.
- [Peters et al. 2011] Peters, J.; Mooij, J.; Janzing, D.; and Schölkopf, B. 2011. Identifiability of causal graphs using functional models. In *Proceedings of the 27th Conference on Uncertainty in Artificial Intelligence, UAI 2011*, 589–598. Corvallis: AUAI Press.
- [Peters et al. 2014] Peters, J.; Mooij, J. M.; Janzing, D.; and Schölkopf, B. 2014. Causal discovery with continuous additive noise models. *The Journal of Machine Learning Research* 15(1):2009–2053.
- [Scutari 2009] Scutari, M. 2009. Learning bayesian networks with the bnlearn r package. *arXiv preprint arXiv:0908.3817*.
- [Shimizu et al. 2006] Shimizu, S.; Hoyer, P. O.; Hyvärinen, A.; and Kerminen, A. 2006. A linear non-gaussian acyclic model for causal discovery. *Journal of Machine Learning Research* 7(Oct):2003–2030.
- [Singh 1997] Singh, M. 1997. Learning bayesian networks from incomplete data. In *Proceedings of the fourteenth national conference on artificial intelligence and ninth con-*



ference on *Innovative applications of artificial intelligence*, 534–539. AAAI Press.

[Spirtes, Glymour, and Scheines 2000] Spirtes, P.; Glymour, C.; and Scheines, R. 2000. Causation, prediction, and search. adaptive computation and machine learning.

[Stekhoven and Bühlmann 2011] Stekhoven, D. J., and Bühlmann, P. 2011. Missforestnon-parametric missing value imputation for mixed-type data. *Bioinformatics* 28(1):112–118.

[Strobl, Visweswaran, and Spirtes 2018] Strobl, E. V.; Visweswaran, S.; and Spirtes, P. L. 2018. Fast causal inference with non-random missingness by test-wise deletion. In *International Journal of Data Science and Analytics*, volume 6, 47–62. Springer.

[Sulik, Newlands, and Long 2017] Sulik, J. J.; Newlands, N. K.; and Long, D. S. 2017. Encoding dependence in bayesian causal networks. *Frontiers in Environmental Science* 4:84.

[Tu et al. 2019] Tu, R.; Zhang, C.; Ackermann, P.; Mohan, K.; Kjellström, H.; and Zhang, K. 2019. Causal discovery in the presence of missing data. In *The 22nd International Conference on Artificial Intelligence and Statistics*, 1762–1770.

[Van den Broeck et al. 2015] Van den Broeck, G.; Mohan, K.; Choi, A.; Darwiche, A.; and Pearl, J. 2015. Efficient algorithms for bayesian network parameter learning from incomplete data. In *Proceedings of the 31st Conference on Uncertainty in Artificial Intelligence (UAI)*, 161.

[Wang et al. 2017] Wang, Y.; Solus, L.; Yang, K.; and Uhler, C. 2017. Permutation-based causal inference algorithms with interventions. In *Advances in Neural Information Processing Systems*, 5822–5831.

[White, Royston, and Wood 2011] White, I. R.; Royston, P.; and Wood, A. M. 2011. Multiple imputation using chained equations: issues and guidance for practice. *Statistics in medicine* 30(4):377–399.

[Xie and Chen 2017] Xie, S., and Chen, Z. 2017. Anomaly detection and redundancy elimination of big sensor data in internet of things. *arXiv preprint arXiv:1703.03225*.

[Yoon, Jordon, and Schaar 2018] Yoon, J.; Jordon, J.; and Schaar, M. 2018. Gain: Missing data imputation using generative adversarial nets. In *International Conference on Machine Learning*, 5675–5684.

[Yu et al. 2019] Yu, Y.; Chen, J.; Gao, T.; and Yu, M. 2019. Dag-gnn: Dag structure learning with graph neural networks. In *International Conference on Machine Learning*, 7154–7163.

[Zhang et al. 2016] Zhang, K.; Wang, Z.; Zhang, J.; and Schölkopf, B. 2016. On estimation of functional causal models: general results and application to the post-nonlinear causal model. *ACM Transactions on Intelligent Systems and Technology (TIST)* 7(2):13.

[Zheng et al. 2018] Zheng, X.; Aragam, B.; Ravikumar, P. K.; and Xing, E. P. 2018. Dags with no tears: Continuous optimization for structure learning. In *Advances in Neural Information Processing Systems*, 9472–9483.